Two Distinct Regions in a Yeast Myosin-V Tail Domain Are Required for the Movement of Different Cargoes

Natalie L. Catlett, Jason E. Duex, Fusheng Tang, and Lois S. Weisman

Department of Biochemistry, University of Iowa, Iowa City, Iowa 52242

Abstract. The *Saccharomyces cerevisiae* myosin-V, Myo2p, is essential for polarized growth, most likely through transport of secretory vesicles to the developing bud. Myo2p is also required for vacuole movement, a process not essential for growth. The globular region of the myosin-V COOH-terminal tail domain is proposed to bind cargo. Through random mutagenesis of this globular tail, we isolated six new single point mutants defective in vacuole inheritance, but not polarized growth. These point mutations cluster to four amino acids in an 11-amino acid span, suggesting that this region is important for vacuole movement. In addition, through characterization of *myo2-ΔAflII*, a deletion of amino acids 1,459–1,491, we identified a second region of the globular tail specifically required for polarized growth. Whereas this mutant does not support growth, it complements the vacuole inheritance defect in *myo2-2* (G1248D) cells. Moreover, overexpression of the *myo2-ΔAflII* globular tail interferes with vacuole movement, but not polarized growth. These data indicate that this second region is dispensable for vacuole movement. The identification of these distinct subdomains in the cargo-binding domain suggests how myosin-Vs can move multiple cargoes. Moreover, these studies suggest that the vacuole receptor for Myo2p differs from the receptor for the essential cargo.

Key words: organelle movement • vacuole • molecular motor • Myo2p • *Saccharomyces cerevisiae*

Introduction

Myosin-V is an actin-based motor protein involved in polarized organelle movement. Analysis of myosin-V mutants in a variety of organisms suggests it is a multifunctional motor, involved in the transport of several cargo organelles. Loss of myosin Va in humans (Griscelli syndrome) or mice (*dilute*) causes lightened pigmentation and neurological defects, including seizures (Mercer et al., 1991; Pastural et al., 1997; Mancini et al., 1998). Analysis of *dilute* mutants suggests that the pigmentation defect is due to impaired transport of melanosomes, pigment-containing lysosomal organelles, to the periphery of melanocytes (Provance et al., 1996; Wei et al., 1997). The neurological defects may be caused by the absence of smooth ER from the dendritic spines of brain Purkinje cells (Takagishi et al., 1996). In addition, as Myosin-Va associates with a subset of synaptic vesicles (Prekeris and Terrian, 1997; Evans et al., 1998; Bridgman, 1999), defects in synaptic vesicle transport may contribute to the observed neurological defects. Griscelli syndrome patients also suffer from immune dysfunction, presumably due to impaired transport of additional, currently unidentified cargo organelles (Pastural et al., 1997). These organelles likely include lysosomal organelles, as lysosomal disorders like Chediak-Higashi syndrome affect both pigmentation and immune function, similar to Griscelli syndrome (for review see Mancini et al., 1998). Even in a single cell type, myosin-V is likely to move multiple cargoes as evidenced by myosin-Va localization to several organelle types in melanocytes by immunoelectron microscopy (Nascimento et al., 1997).

The *Saccharomyces cerevisiae* myosin-V, Myo2p, is an essential protein required for polarized growth and the transport of secretory vesicles (Johnston et al., 1991; Govindan et al., 1995; Pruyne et al., 1998; Reck-Peterson et al., 1999; Schott et al., 1999). Loss of Myo2p function causes yeast to cease budding and accumulate small vesicles in the mother cell (Govindan et al., 1995; Reck-Peterson et al., 1999). Also consistent with a general role in secretory vesicle transport, the secretory vesicle protein Sec4p delocalizes from sites of polarized secretion after loss of Myo2p function (Walch-Solimena et al., 1997; Reck-Peterson et al., 1999; Schott et al., 1999). A related essential role of Myo2p is the transport of vesicles containing cell wall components to sites of polarized growth. Loss of Myo2p function causes the chitin synthase Chs3p to delocalize, and chitin deposi-

Address correspondence to Lois S. Weisman, Department of Biochemistry, University of Iowa, Iowa City, IA 52242. Tel.: (319) 335-8581. Fax: (319) 335-9570. E-mail: lois-weisman@uiowa.edu

tion to shift from the incipient bud site and bud neck to the entire cell surface (Johnston et al., 1991; Santos and Snyder, 1997). In addition to its essential cargo(es), Myo2p is involved in transport of the lysosome-like vacuole during cell division. A subset of *myo2* mutants is defective for the directed movement of a portion of the mother cell vacuole into the bud, and thus new daughter cells do not inherit a vacuole (Hill et al., 1996; Catlett and Weisman, 1998). The detection of both essential and nonessential cargo in a single cell presents the opportunity to dissect the roles of a myosin-V in two distinct transport processes.

Although many potential cargoes for class V myosins have been identified, little is known about how myosin-V binds to these organelles. The myosin-V tail domain contains both coiled-coil regions mediating dimerization and a globular domain thought to mediate cargo binding and subcellular localization (Cheney et al., 1993). A few lines of evidence support this hypothesis for function of the globular region. First, the tail domain alone localizes similarly to full-length myosin-V (Wu et al., 1998; Bridgman, 1999; Reck-Peterson et al., 1999). Moreover, overexpression of the tail domain causes dominant negative phenotypes suggestive of competition for binding sites with the full-length myosin-V. In yeast, overexpression of the Myo2p globular tail causes accumulation of vesicles and a loss of polarized growth similar to the temperature-sensitive *myo2-66* mutant at restrictive temperatures (Reck-Peterson et al., 1999). Similarly, in melanocytes, overexpression of myosin-V tail constructs causes a perinuclear melanosome distribution similar to that seen in *dilute* cells (Wu et al., 1998).

Characterization of myosin-V mutations has also provided support for a role of the globular tail domain in localization and cargo binding. In mice, multiple *dilute* mutants have mutations mapping to the globular tail (Huang et al., 1998). Interestingly, some of these mutations affect tissue-specific splicing and the resulting absence of the melanocyte-specific dilute isoform causes pigmentation, but not neurological defects (Huang et al., 1998). In yeast, deletion of the Myo2p globular tail domain is lethal, indicating that this domain is absolutely required for the essential function of Myo2p (Catlett and Weisman, 1998). Furthermore, cells containing *myo2-2*, a single point mutation (G1248D) in the globular tail domain, retain the essential functions of Myo2p, yet display a severe vacuole inheritance defect (Catlett and Weisman, 1998). This mutation dramatically lowers the association of Myo2p with isolated vacuoles, implying that the vacuole inheritance defect is due to poor association of the mutant Myo2p with the vacuolar receptor (Catlett and Weisman, 1998). In addition, the mutant Myo2p does not concentrate at sites of polarized growth, the primary site of Myo2p localization in wild-type cells (Catlett and Weisman, 1998). The defects in localization to the vacuole and concentration at sites of polarized growth seen in this tail mutant strongly argue for a role of the tail domain in localization. However, little is known about the regions of the globular tail required for specific functions.

In this report, we further investigate the role of the globular tail domain in Myo2p function. We performed random mutagenesis of this domain to identify additional mutations with specific effects on vacuole inheritance. Unexpectedly, these mutations clustered to four amino acids in an 11-amino acid stretch, thus defining a putative vacuole-binding region. In addition, we identify a region of the tail dispensable for vacuole inheritance, but required for the essential function of Myo2p. We previously reported *myo2-*Δ*AflII*, a 33-amino acid deletion that is stably expressed yet cannot perform the essential function(s) of Myo2p (Catlett and Weisman, 1998). Here, we report the surprising result that this allele is functional for vacuole inheritance. Moreover, whereas overexpression of the wild-type globular tail domain is toxic to the cell, overexpression of the globular tail domain with this deletion (tail-Δ*AflII*) has little effect on cell growth, yet severely inhibits vacuole inheritance. These results suggest the presence of two distinct cargo-binding regions on the Myo2p tail, one required for the essential function(s) and one required for vacuole inheritance.

Materials and Methods

Yeast Strains and Media

Yeast strains are shown in Table I. LWY2949 and LWY5745 were generated by transforming pΔM::TRP1 into a wild-type diploid as described (Lillie and Brown, 1994), then transforming with pMYO2 (YCp50-based plasmid containing *MYO2*; Johnston et al., 1991), sporulating, and dissecting tetrads. *myo2*Δ strains containing plasmids other than pMYO2 as the sole copy of *MYO2* were generated by transforming pRS413 (low copy, HIS3; Sikorski and Hieter, 1989) containing the appropriate *myo2* allele into LWY2949 or LWY5745, and selecting on 5-fluoroorotic acid (5-FOA)-containing medium for cells no longer containing the pMYO2 plasmid. To make LWY5648, LWY2949 carrying pRS413-MYO2 (Catlett and Weisman, 1998) was transformed with the URA3-selected plasmid pRS416-MYO2-PEP4, and were then grown on rich media and checked for histidine auxotrophy.

Yeast extract-peptone-dextrose (1% yeast extract, 2% peptone, 2% dextrose; YEPD)[1], synthetic complete (SC) lacking the appropriate supplement(s), and 5-FOA media were made as described (Kaiser et al., 1994). Unless stated otherwise, SC medium contained 2% dextrose. When indicated, SC medium without uracil was supplemented with 0.5% casamino acids (Difco). Standard yeast genetic techniques were used (Kaiser et al., 1994).

Plasmids

For pRS416-MYO2-PEP4, a ClaI fragment containing *MYO2* was subcloned from pMYO2 into pRS416 (Sikorski and Hieter, 1989) to generate pRS416-MYO2. *PEP4* was amplified from pBVH117 (van den Hazel et al., 1993) by PCR using primers KpnI-PEP41 (5′-CGG**GGTACC**GAGCTC-CTCAATTGTATTTG-3′) and KpnI-PEP42 (5′-CGG**GGTACC**CTCG-GCCGCATCATGGG-3′) to generate KpnI sites (underlined in bold) on both ends and cloned into the KpnI site of pRS416-MYO2 to generate pRS416-MYO2-PEP4. For pMYO2-tail, DNA encoding amino acids 1,113–1,574 of Myo2p was PCR amplified from pMYO2 to add a 5′ KpnI site and a 3′ SacI site using primers MYO2-Kpn1F (5′-GCCG**GGTAC-C**CAACAATATGATGCTTG-3′) and YCP50 3′ (5′-GCCG**GAGCTC**-CTGTGATAAACTACCGC-3′). This fragment was then ligated into pYES2 (yeast expression vector with GAL1 promoter and URA3 marker; Invitrogen) at the KpnI and SacI sites. The 99-bp AflII fragment encoding amino acids 1,459–1,491 of Myo2p was removed from pMYO2-tail to generate pNLC22. For pNLC59 (pMYO2-tail, N1304D) and pNLC60 (pMYO2-tail2), BamHI–PstI DNA fragments encoding amino acids 1,113–1,574 of Myo2p with or without the N1304D point mutation were ligated into the BamHI and PstI sites of pYES2. For pNLC27, DNA encoding amino acids 1,113–1,574 (with the 1,459–1,491 deletion) of Myo2p was

[1]*Abbreviations used in this paper:* CPY, carboxypeptidase Y; FM4-64, *N*-(3-triethylammoniumpropyl)-4-(6(4-(diethylamino)phenyl)hexatrienyl) pyridinium dibromide; PrB, proteinase B; YEPD, 1% yeast extract, 2% peptone, 2% dextrose.

Table I. Strains Used in this Study

Strain	Genotype	Source
LWY7235	*MATa, ura3-52, leu2-3,112, his3-Δ200, trp1-Δ901, lys2-801, suc2-Δ9*	Bonangelino et al., 1997
LWY5518	*MATa, ura3-52, leu2-3,112, his3-Δ200, trp1-Δ901, lys2-801, suc2-Δ9, pep4-Δ1137, myo2-2*	This study
LWY2949	*MATα, ura3-52, leu2-3,112, his3-Δ200, trp1-Δ901, lys2-801, suc2-Δ9, pep4-Δ1137, myo2Δ::TRP1, pMYO2*	This study
LWY5475	*MATa, ura3-52, leu2-3,112, his3-Δ200, trp1-Δ901, lys2-801, suc2-Δ9, myo2Δ::TRP1, pMYO2*	This study
LWY5648	*MATα, ura3-52, leu2-3,112, his3-Δ200, trp1-Δ901, lys2-801, suc2-Δ9, pep4-Δ1137, myo2Δ::TRP1,* pRS416-MYO2-PEP4	This study

amplified from pNLC22 by PCR to add a 5′ BamHI site using primers MYO2-Bam3F (5′-CGC**GGATCC**AACAATATGATGCTTG-3′) and YCP50 3′ (see above), and was then ligated into the BamHI and SacI sites of pVT102-U (ADH driven yeast expression vector with URA3 marker; Vernet et al., 1987). For pNLC56 and pNLC57, BamHI–SalI fragments encoding amino acids 1,113–1,574, Δ1,459–1,491 of Myo2p with G1248D or N1304D point mutations were ligated into the BamHI and XhoI sites of pVT102-U. pNLC44 (HA epitope-tagged *myo2-ΔAflII*) was constructed by subcloning a 1-kb EcoRI–AflII fragment from a YIp5 vector containing a PvuII–ClaI Myo2p fragment with a single HA epitope inserted at the BglII site in the tail domain (Reck-Peterson et al., 1999) into pNLC39 (pRS413-MYO2 with the EcoRI site in the polylinker removed by Klenow fill in) with the corresponding EcoRI–AflII MYO2 fragment removed. This procedure had the dual effect of introducing the HA tag and removing the 99-bp AflII fragment. pNLC45 (HA epitope-tagged myo2-tail-ΔAflII) was constructed by PCR-amplifying a *myo2* tail fragment from pNLC44 using primers MYO2-Bam3F and YCP50 3′ (see above), digesting with BamHI and SalI, and ligating to pVT102-U at the BamHI and XhoI sites.

Random Mutagenesis of MYO2

To generate *myo2* mutants, the *MYO2* tail region from pRS426-MYO2 was PCR amplified with Taq polymerase (Boehringer) following the manufacturer's instructions. Primers used were MYOL (5′-CGGAGACTTG-CAAAACG-3′) and MYOR (5′-TGTGGAATTGTGAGCGG-3′). This product was purified using QIAquick gel extraction kit (QIAGEN Inc.) after agarose gel electrophoresis. pMYE (Catlett and Weisman, 1998) was linearized with EcoRI and phosphatase treated. Linearized pMYE was cotransformed with the PCR-amplified *MYO2* tail into LWY2949 cells containing pRS416-MYO2-PEP4. Transformants were replica plated onto 5-FOA–containing media to remove pRS416-MYO2-PEP4. The plates were then replica plated to YEPD and assayed for carboxypeptidase Y (CPY) activity as described (Jones, 1991) with minor modifications. In brief, each plate was overlayed with a mixture of 2 ml of 2 mg/ml *N*-acetyl-DL-phenylalanine Δ-napthyl ester (Sigma-Aldrich) in dimethylformamide and 2 ml 0.6% molten agarose. After the agarose mixture solidified, 5 ml of 0.5 mg/ml Fast Garnet GBC (95%; Sigma-Aldrich) in 0.1 M Tris, pH 7.3–7.5 was added to each plate. After color development was complete (~10 min), plates were washed with sterile water and CPY^- (white) colonies selected by stabbing through the agarose overlay and restreaking onto fresh media. Resultant colonies were individually screened by microscope for vacuole inheritance defects. Plasmids were isolated from colonies displaying vacuole inheritance defects and retransformed into LWY2949.

Protein Sequence Analysis

Sequence data was obtained through the National Center for Biotechnology Information (http://www.ncbi.nlm.nih.gov), except data for *Candida albicans* and *Cryptococcus neoformans* was obtained from the Stanford DNA Sequencing and Technology Center website at http://www-sequence.stanford.edu/group/candida and http://www-sequence.stanford.edu/group/C.neoformans, respectively. Sequencing of *Candida albicans* was accomplished with the support of the NIDR and the Burroughs Wellcome Fund. Protein sequence alignments were performed using ClustalW (Thompson et al., 1994; http://pbil.ibcp.fr/NPSA/npsa_clustalw.html). Secondary structure predictions were performed using SOPMA (Geourjon and Deleage, 1995) or PHD (Rost and Sander, 1994; available at: http://pbil.ibcp.fr/NPSA/npsa_sopma.html and http://pbil.ibcp.fr/NPSA/npsa_phd.html).

FM4-64 Labeling of Vacuoles

Vacuoles were labeled in vivo with *N*-(3-triethylammoniumpropyl)-4-(6(4-(diethylamino)phenyl)hexatrienyl) pyridinium dibromide (FM4-64; Molecular Probes) essentially as described (Hill et al., 1996). In brief, a 1 mg/ml stock solution of FM4-64 in DMSO was added to log phase cultures for a final concentration of 40 μM. Cultures labeled in synthetic medium were buffered in 20 mM Pipes, pH 6.8. After 1–1.5 h of labeling, cells were washed and were then label-chased in fresh liquid medium.

Immunofluorescence

Indirect immunofluorescence was performed essentially as described (Hill et al., 1996). Log phase cells were fixed for 2 h by addition of 37% formaldehyde in the culture medium to a final concentration of 3.7%. The fixed cells were resuspended in SPB (1.2 M sorbitol, 0.1 M potassium phosphate, pH 6.5, 1% Δ-mercaptoethanol) and the cell wall was removed by digestion with oxalyticase (Enzogenetics). The resultant spheroplasts were immobilized on 8-well slides (ICN) coated with polyethyleneimine and incubated with PBS containing 0.5% NP-40 and 1% BSA to block nonspecific binding. For detection of actin, the Myo2p motor domain, and HA-tail-Δ*AflII*, cells were treated for 6 min in −20°C methanol and then 30 s in −20°C acetone. In general, primary antibody incubations were overnight and fluorophore-labeled secondary antibody incubations were 1 h. Myo2p was detected with affinity-purified rabbit polyclonal anti-Myo2p tail antiserum (0.8 μg/ml; Reck-Peterson et al., 1999) or anti-Myo2p motor domain antiserum (0.25 μg/ml; Reck-Peterson et al., 1999), followed by Oregon green 488-labeled goat anti-rabbit IgG (1:400). Actin was detected with affinity-purified goat antiyeast actin antiserum at a 1:200 concentration, followed by Alexa Fluor 488-conjugated donkey anti–goat IgG (3.75 μg/ml; Molecular Probes). HA-tail-Δ*AflII* was detected with mouse monoclonal anti-HA IgG (BabCo; 1:1,000), followed by lissamine rhodamine–conjugated donkey anti–mouse IgG (1:200; Jackson ImmunoResearch Laboratories). Vacuole membranes were labeled with affinity-purified rabbit polyclonal anti-Vac8p antibody (Wang et al., 1998), followed by Oregon green 488-labeled goat anti–rabbit IgG (1:400).

Detection of HA-*myo2*-Δ*AflII* was performed as described with minor modifications (Berkower et al., 1994). Cells were harvested, resuspended in 0.1 M sodium phosphate buffer, pH 6.5, containing 3.7% formaldehyde, and fixed for 45 min. The fixed cells were spheroplasted and adhered to slides as described above. Mouse monoclonal anti-HA IgG (BabCo) was used at a 1:100 concentration and detected with 1:400 Alexa Fluor 488-conjugated goat anti–mouse IgG (Molecular Probes).

Fluorescence Microscopy

Cells were viewed on an Olympus BX-60 fluorescence microscope using a 100× objective lens. Images were captured with a Hamamatsu ORCA CCD camera controlled with IP spectrum software (Scanalytics Inc.). Images were saved as 16-bit TIFF files and processed using Adobe Photoshop™.

Confocal images for HA-tail-ΔAflII localization studies were obtained with an MRC-1024 laser scanning confocal (BioRad) mounted on a Nikon Optiphot microscope. For each field, a z-series of 0.5-μm slices was scanned and exported as 8-bit TIFF files.

Cell Fractionation

Cell fractionation was performed as described (Catlett and Weisman, 1998; Wang et al., 1998) except cells were grown in synthetic medium supplemented with 0.5% casamino acids. In brief, cells grown to mid-log phase were harvested, washed, and resuspended in cold lysis buffer (0.3 M sorbitol, 10 mM Tris, 0.1 M NaCl, 1 mM $MgCl_2$, 1 mM EDTA, pH 7.5) plus 1 mM phenylmethylsulfonyl fluoride and 1× complete protease inhibitor mixture (Boehringer). Cells were vortexed with glass beads 10 × 30 s. The resultant extract was cleared by centrifugation at 500 *g* for 5 min to generate the S0.5. Then, the S0.5 supernatant was centrifuged at 13,000 *g* for 10

min to generate the P13 pellet and S13 supernatant. The S13 was centrifuged at 100,000 *g* to generate the P100 pellet and S100 supernatant. Equal OD_{600} units of cell lysates (0.25 OD_{600}) were separated on a 10% polyacrylamide SDS gel. Proteins were transferred to Hybond ECL nitrocellulose (Amersham Pharmacia Biotech) at 30 V for 22–24 h.

Vacuoles were isolated on a Ficoll flotation gradient as described (Catlett and Weisman, 1998), except cells were grown in synthetic medium lacking uracil and supplemented with 0.5% casamino acids.

Myo2p was detected by incubating nitrocellulose membranes overnight with goat anti-Myo2p antiserum (1:2,500), then with HRP-conjugated donkey anti–goat IgG (1:5,000; Jackson ImmunoResearch Laboratories) for 1 h. Bands were visualized using ECL (Amersham Pharmacia Biotech). To make goat anti-Myo2p antiserum, GST-Myo2p tail fusion protein was prepared from plasmid RPB50 (pGEX-5X-1-Myo2 tail; Reck-Peterson et al., 1999) and antibody was generated in goats by Elmira Biologicals.

Results

An 11-Amino Acid Region of the Globular Tail Is Critical for Vacuole Inheritance

myo2-2 (G1248D), a point mutation in the globular tail domain of Myo2p, causes defects in vacuole inheritance and association with the vacuole (Catlett and Weisman, 1998). To identify additional regions of the Myo2p globular tail important for vacuole binding, we mutagenized this domain and isolated alleles defective in vacuole segregation. To identify these mutants, we adapted a screen using the loss of vacuolar protease activation as a measure of vacuole inheritance (Gomes de Mesquita et al., 1996; Fig. 1 A). Most vacuolar proteases are synthesized as inactive precursors and then proteolytically activated in the vacuole. Proproteinase B (proPrB) is activated by proteinase A (PrA), encoded by the *PEP4* gene, and also by active PrB (Jones, 1991). In wild-type cells, proPrB activation continues for many generations after the loss of the *PEP4* gene, due to PrB that is partitioned with the vacuole (Jones, 1991; Gomes de Mesquita et al., 1996). In contrast, in vacuole segregation mutants, daughter cells must synthesize a vacuole de novo and thus do not inherit active PrB. Active PrB can be monitored indirectly through a red/white plate assay for activity of a third protease, CPY (Jones, 1991). This allows the rapid screening of thousands of candidates for vacuole inheritance defects by transiently expressing the *PEP4* gene and testing for CPY activity.

Of ~40,000 transformants screened for CPY activity, 53 CPY deficient candidates were selected for further study. These were labeled with the vacuole-specific dye FM4-64 (Vida and Emr, 1995), the label chased for at least one cell-doubling time, and screened by microscope for vacuole inheritance defects. 24 candidates displayed severe vacuole inheritance defects; few segregation structures extending from the mother vacuole into the bud were observed, and most buds did not contain a labeled vacuole inherited from the mother cell (Fig. 1 C).

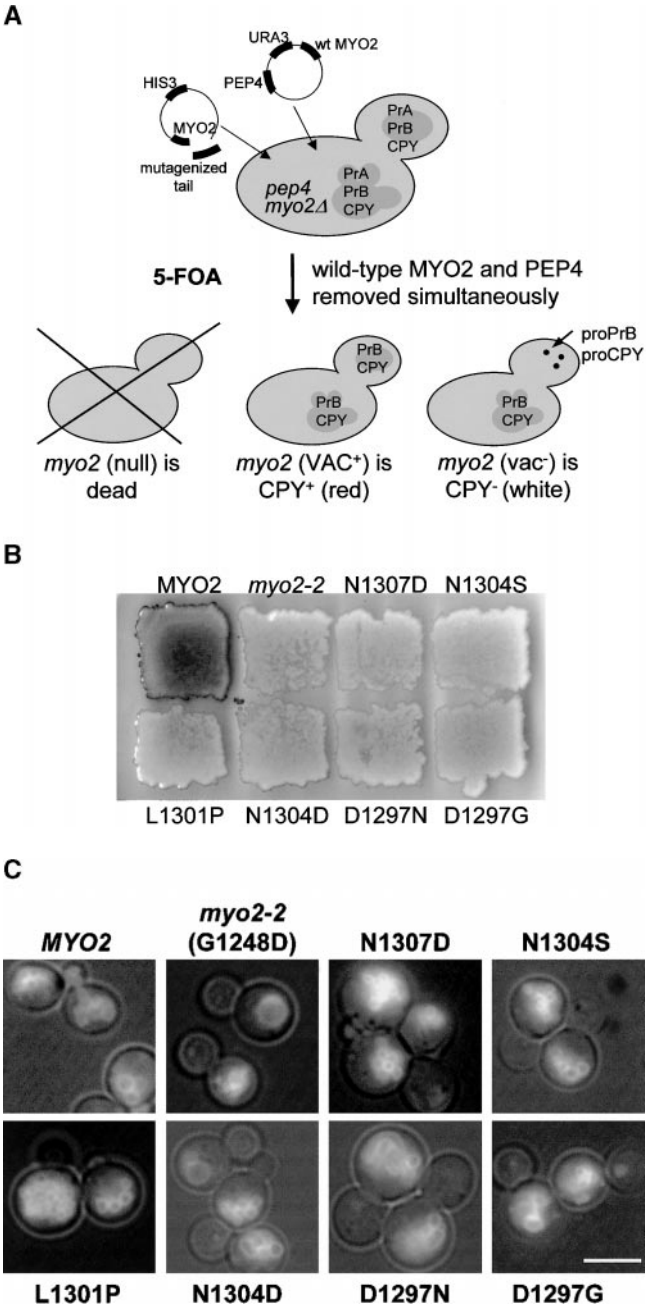

Figure 1. Loss of CPY activation after removal of *PEP4* as a screen for *myo2* vacuole inheritance mutants. In wild-type cells, if *PEP4* is lost, proPrB and proCPY activation will continue for many generations due to PrB that is partitioned with the vacuole. A, The *MYO2* globular tail region was amplified by PCR under mutagenic conditions. A linearized, *HIS3 MYO2* plasmid with the tail region deleted (pMYE) was cotransformed with the PCR-amplified fragment into LWY5648 (*myo2*Δ*::TRP1, his3-*Δ*200, ura3-52, pep4-*Δ*1137,* pRS416-MYO2-PEP4). These plasmid fragments recombine in the yeast to form a circular plasmid. Transformants were replica plated to 5-FOA media as a counter-selection for pRS416-MYO2-PEP4, and thus now carry the mutagenized *myo2* as the sole *myo2* and no longer express *PEP4*. Cells carrying a *myo2* gene not competent for its essential function are no longer viable. Next, transformants were replica plated to rich medium (YEPD) and assayed for CPY activity. White (CPY^-) colonies were selected for further study. B, CPY assay of *myo2* point mutants. LWY5648 cells were transformed with pRS413 carrying the indicated *myo2* allele. Transformants were patched onto 5-FOA medium, then replica plated to YEPD and assayed for CPY activity. C, Vacuole labeling of *myo2* point mutants. *myo2*Δ*::TRP1* cells carrying the indicated allele of *MYO2* in pRS413 were grown to log phase in YEPD, 24°C and labeled with the vacuole-specific vital dye FM4-64. After 1 h of labeling, cells were washed, the label chased in fresh media for 3 h, and visualized using transmitted light and a rhodamine filter set. Bar, 5 μm.

A

```
      G      D
      N   P  S  D
1297  DFEALSYNIYN  1307
```

B

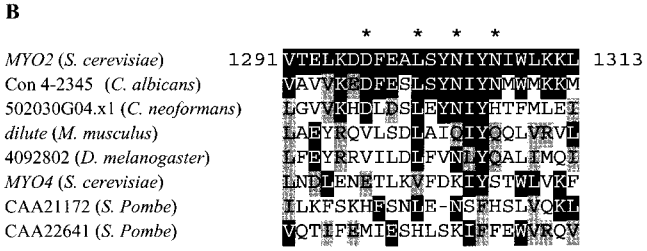

Figure 2. A putative vacuole-binding region in the globular tail domain. A, The Myo2p amino acid sequence from 1,297 to 1,307 is listed with the amino acids affected by point mutations in bold type. Amino acid changes of the mutants are listed above the affected residues. B, Alignment of myosin-V globular tail sequences. Clustal W (Thompson et al., 1994) was used to align myosin-V–related protein sequences from a variety of organisms. The segments aligning with amino acids 1,291–1,313 of Myo2p are shown above. The Myo2p sequence and residues identical to Myo2p are shaded black and similar residues are shaded gray. Asterisks above the Myo2p sequence indicate residues affected by vacuole inheritance mutants.

Table II. Multiple Mutations in myo2 Alleles

Allele	Amino acid changes	Additional phenotypes
*myo2-4**	N1277K K1319E I1475T	Temperature-sensitive growth
myo2-5	T1231S T1274A D1297V‡ I1399M I1498M	
myo2-6	M1114T E1293G L1294Q N1307D§ F1361S F1404L S1506T	Myo2p localization defect
myo2-7	F1224L P1246A D1297V‡	Myo2p localization defect

*Each of these mutations was reintroduced individually. None caused the indicated phenotypes.
‡This mutation causes defects in vacuole inheritance when introduced as a single point change.
§This mutation was isolated as a single point change in the present screen (Catlett and Weisman, 1998).

The mutant *myo2* plasmid was rescued from these alleles and the mutagenized region of the tail sequenced. The 20 plasmids that contained a single point change represented seven distinct alleles (Figs. 1 B and 2 A). One of these, G1248D, is *myo2-2*. The other six single point mutations cluster to four amino acids in an 11-amino acid stretch (D1297, L1301, N1304, and N1307).

Previously, we generated *myo2-4*, *myo2-5*, *myo2-6*, and *myo2-7* through PCR-based mutagenesis (Catlett and Weisman, 1998; Hutchings, N., and L.S. Weisman, unpublished). Sequencing these alleles revealed three to seven amino acid changes each, thus obscuring which changes specifically affect vacuole movement (Table II). Interestingly, *myo2-5*, *myo2-6*, and *myo2-7* each contain a change in one of the four amino acids identified above. *myo2-4* does not contain a change in this region. However, when its three point changes were reintroduced individually by site-directed mutagenesis, none of these changes alone caused a vacuole inheritance defect. The reoccurrence of G1248D and mutations in these four amino acids suggests that this region is critical for Myo2p function in vacuole inheritance.

We used several secondary structure prediction programs to further characterize this region. Several secondary structure prediction algorithms predict this region to be α-helical. SOPMA, a method using consensus prediction from alignments of related sequences (Geourjon and Deleage, 1995), predicts a helix from amino acids 1,283–1,324. Similarly, a second algorithm, PHD (Rost and Sander, 1994), predicts a helix at amino acids 1,289–1,319. Strikingly, the amino acid residues changed in our vacuole inheritance mutants are spaced three or four amino acids apart, so as to fall on one face of this predicted helix. We aligned Myo2p with a number of other myosin-V sequences to determine the evolutionary conservation of this newly identified vacuole-binding region (Fig. 2 B). This region is conserved in Myo2p-like sequences identified by the *C. albicans* and *C. neoformans* sequencing projects, suggesting that these predicted proteins may also have a role in vacuole movement. In addition, vertebrate myosin-Va protein sequences have similarity or identity to three of the four amino acids forming the proposed vacuole-binding face in Myo2p. This region is much less conserved in Myo4p. However, this lack of conservation is not surprising given that Myo4p is not required for vacuole inheritance (Hill et al., 1996) and instead has a role in RNA transport (Long et al., 1997). This region was also only weakly similar in both *Schizosaccharomyces pombe* myosin-V sequences.

Myo2p Is Partially Mislocalized in the New myo2 Mutant Alleles

In wild-type cells, Myo2p concentrates at sites of polarized growth, including the presumptive bud site, the tips of small buds, the mother/bud neck before cytokinesis, and the tips of mating factor-induced projections. In contrast, myo2-2p does not concentrate at any of these sites (Catlett and Weisman, 1998). Thus, this polarized concentration is not required for polarized growth, but may have some correlation with vacuole inheritance. To examine the localization of Myo2p in the new *myo2* mutants, we performed indirect immunofluorescence using an antibody directed against the globular tail domain of Myo2p (Reck-Peterson et al., 1999; Fig. 3). All of the mutants displayed some polarized distribution of Myo2p; however, the intensity of

the staining was frequently fainter than that seen in wild-type populations, and not all cells displayed this polarization. The percentage of cells displaying polarized Myo2p was quantitated in three representative mutants, D1297G, N1304D, and N1307D. Polarization of Myo2p in unbudded and small-budded cells was assessed in random fields. In each of the mutants tested, slightly more than half of the cells counted displayed polarized concentrations of Myo2p (Fig. 3 B). In contrast, nearly all of the wild-type and almost none of the *myo2-2* cells had polarized Myo2p staining. A similar partial loss of polarized localization as compared with wild-type cells was seen in medium-budded cells and cells about to undergo cytokinesis (Fig. 3 A, and data not shown). A similar staining pattern was observed using antibody directed against the Myo2p motor domain (Reck-Peterson et al., 1999; data not shown). Localization of the mutant Myo2p to the tips of mating pheromone-induced projections (shmoos) was investigated by treating cells with 10 μg/ml α-factor for 2 h before fixing and processing for immunofluorescence. In the three mutant strains tested, slightly less than half of the cells with prominent projections showed polarized Myo2p (data not shown).

This partial Myo2p localization defect suggests that amino acids 1,297–1,307, affected in these mutants, are more specifically involved in vacuole inheritance than G1248, which when altered in *myo2-2* completely disrupts Myo2p polarization, as well as abolishing vacuole inheritance.

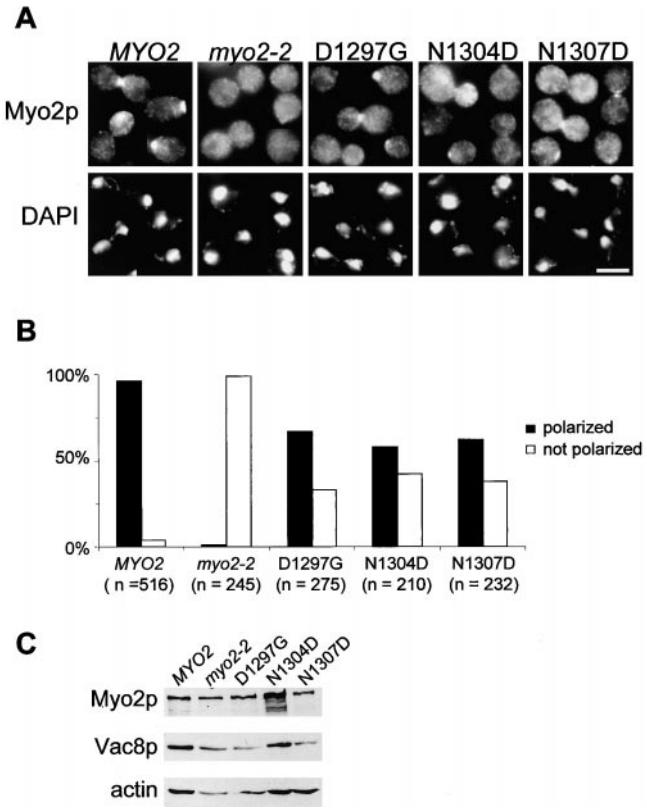

Figure 3. Immunolocalization of mutant Myo2p. A, *myo2Δ::TRP1* cells carrying the indicated allele of *MYO2* in pRS413 were grown overnight in YEPD at 24°C, fixed, processed for immunofluorescence, and stained using anti-Myo2p tail-domain antibody and DAPI. Bar, 5 μm. B, Unbudded and small-budded cells in random fields were assessed for polarized localization of Myo2p. C, Mutant Myo2p levels are comparable to wild-type levels. Cell extracts were generated from each strain above. Equal OD_{600} units were separated by SDS-PAGE, and were then transferred to nitrocellulose and probed using antibodies against the Myo2p motor domain, Vac8p, and yeast actin.

myo2-ΔAflII Can Support Vacuole Inheritance in myo2-2 Cells

myo2-ΔAflII (pMYA) is a deletion of amino acids 1,459–1,491 of the Myo2p tail that is stably expressed, but cannot perform the essential functions of Myo2p (Catlett and Weisman, 1998). To determine if *myo2-ΔAflII* is functional for vacuole segregation, we introduced plasmids carrying this and other *myo2* alleles into LWY5518 (*myo2-2*). As *myo2-2* is defective in vacuole segregation, but completely viable (Catlett and Weisman, 1998), introduction of inviable *myo2* deletions into *myo2-2* allows assessment of their capacity to move the vacuole.

Transformants were labeled with FM4-64 as described above. All cells with a labeled vacuole in the mother cell were scored for vacuole staining in the bud (Fig. 4 B). *myo2-2* cells (LWY5518) carrying the vector alone (pRS413) or pMYE (pRS413-*myo2-Δtail*) showed severe defects in vacuole inheritance. Cells carrying pMYA (pRS413-*myo2-ΔAflII*) displayed almost wild-type vacuole inheritance (Fig. 4, A and B). 86% of cells counted contained vacuole label in the bud, and many had segregation structures connecting the mother and bud vacuoles. In addition, we examined the effect of pNLC1 (pRS413-*myo2-2*) and pRS413- *myo2-6* (Catlett and Weisman, 1998) on vacuole inheritance in *myo2-2* cells. Neither plasmid had a significant effect, suggesting that merely expressing more mutant Myo2p cannot account for the suppression of the *myo2-2* vacuole inheritance defects by pMYA (pRS413-*myo2-ΔAflII*).

It is possible that the suppression of the *myo2-2* vacuole inheritance defect by *myo2-ΔAflII* requires heterodimer formation between the two mutants. Myosin-Vs, including Myo2p, dimerize through the coiled-coil region of the tail (Cheney et al., 1993; Beningo et al., 2000). Thus, when two alleles are expressed in a single cell, heterodimerization seems inevitable. In this case, one heavy chain (*myo2-ΔAflII*) would supply an intact vacuole-binding site, and one (*myo2-2*) would supply the binding site for the essential cargo. However, it is also likely that *myo2-ΔAflII* homodimers can move the vacuole. Indeed, normal movement of a given cargo may require intact binding sites on both globular tail domains. Nonetheless, both interpretations are consistent with *myo2-ΔAflII* containing a complete, functional vacuole-binding site.

The myo2-ΔAflII Gene Product Localizes to Sites of Polarized Growth

To determine the localization of the *myo2-ΔAflII* gene product independent of the endogenous Myo2p, we constructed an epitope-tagged *myo2-ΔAflII* with a single HA inserted into the BglII site in the tail domain. This epitope tag is reported not to affect Myo2p function (Reck-Peterson et al., 1999), and the tagged *myo2-ΔAflII* has the same

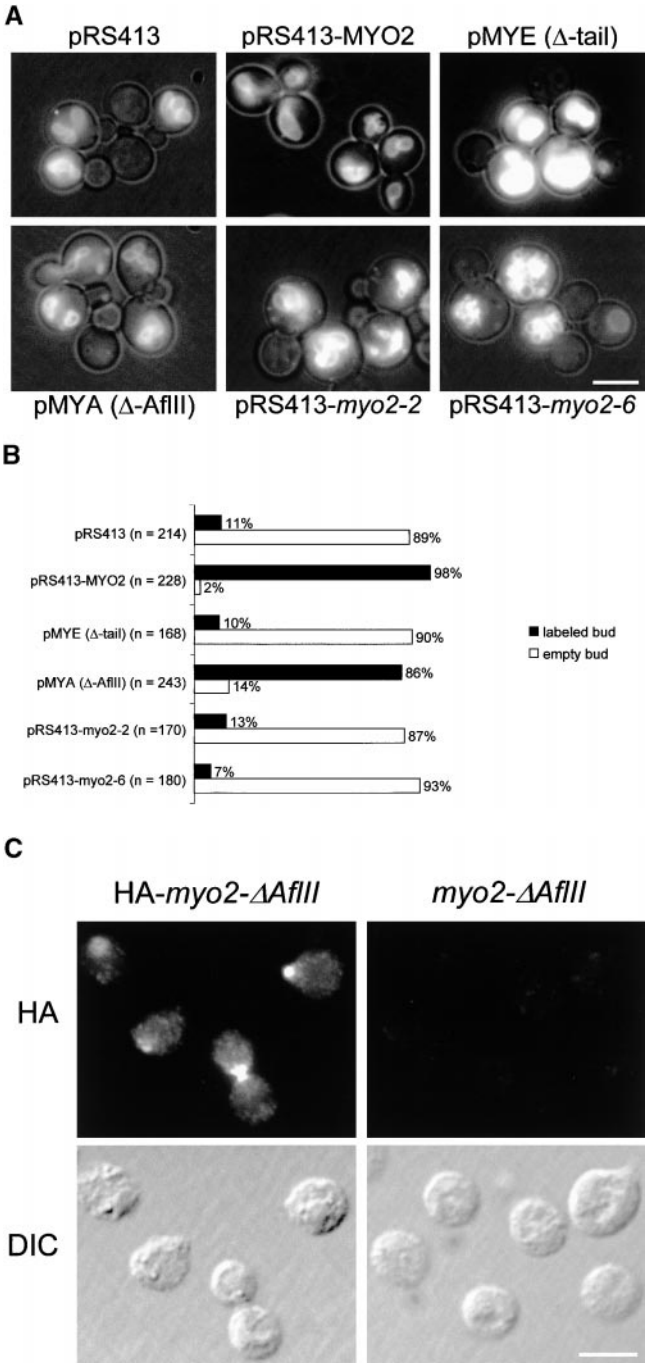

Figure 4. *myo2-ΔAflII* can support vacuole inheritance in *myo2-2* cells. A, LWY5518 (*myo2-2*) cells were transformed with the indicated plasmid. Transformants were grown overnight in selective media, labeled with the vacuole specific dye FM4-64, and the dye chased for approximately one doubling time. B, Quantitation of cells in A. Although *myo-ΔAflII* (pMYA) cannot support the essential functions of *MYO2*, it is functional for vacuole inheritance. C, Immunolocalization of HA-myo2-ΔAflIIp. LWY5518 (*myo2-2*) cells with pMYA (*myo2-ΔAflII*) or pNLC44 (*HA-myo2-ΔAflII*) were grown overnight in selective media at 24°C, fixed, and stained using anti-HA antibody. Bar, 5 μm.

effects on vacuole inheritance as the untagged (data not shown). We performed indirect immunofluorescence using anti-HA antibody on both LWY7235 (*MYO2*) and LWY5518 (*myo2-2*) cells containing pMYA (pRS413-*myo2-ΔAflII*) or pNLC44 (pRS413-HA-*myo2-ΔAflII*). The HA-tagged *myo2-ΔAflII* localizes to the tips of small buds and the presumptive bud site while no HA staining is seen in cells containing the untagged construct (Fig. 4 C). In the *myo2-2* cells, this localization is likely independent of the endogenous myo2-2p, since this protein does not concentrate in these sites of active growth. The polarized localization of the HA-myo2-ΔAflIIp indicates that while the 33-amino acid deletion disrupts the essential function of Myo2p, it does not affect localization.

Overexpression of the myo2-ΔAflII Globular Tail Inhibits Vacuole Inheritance

Overexpression of the Myo2p globular tail domain causes defects in polarized cell growth similar to those seen in *myo2-66* at the nonpermissive temperature (Reck-Peterson et al., 1999). This effect is likely due to competition of the overexpressed tail with the full-length endogenous Myo2p for binding sites on essential cargo(es). Our results above suggest that myo2-ΔAflIIp is unable to interact with essential cargo, yet interaction with the vacuole is intact. Thus, overexpression of the globular tail domain with this deletion might disrupt full-length Myo2p interaction with the vacuole, but not affect the essential functions of Myo2p.

To test this hypothesis, we constructed high copy plasmids with a full-length globular tail domain (pMYO2-tail and pNLC60) and a globular tail domain with the Δ*AflII* deletion (pNLC22), both under the inducible *GAL1* promoter. Western blot analysis confirmed that all tail constructs were expressed at approximately equal levels after induction in galactose-containing media (data not shown). As expected, overexpression of the full-length Myo2p globular tail domain severely affected growth. However, cells overexpressing the tail-Δ*AflII* construct grew similarly to cells with the vector alone (Fig. 5 A). In addition, we constructed a plasmid (pNLC59) for galactose inducible overexpression of the Myo2p tail with the N1304D mutation found to disrupt vacuole inheritance. This construct was expressed similarly to the other tail overexpression constructs (data not shown). This mutant tail disrupts growth, however somewhat less strongly than the wild-type tail (Fig. 5 A).

To examine easily the effects of Myo2p tail-Δ*AflII* overexpression on vacuole inheritance, a plasmid (pNLC27) expressing the tail-Δ*AflII* under the *ADH* promoter was constructed. An HA epitope-tagged version (pNLC45) of this plasmid was also constructed. These constructs allow constitutive expression of Myo2p tail-Δ*AflII* in standard growth conditions. Vacuole inheritance was assessed in wild-type (LWY7235) cells containing pNLC27 (tail-Δ*AflII*), pNLC45 (HA-tail-Δ*AflII*), or the vector alone by labeling with FM4-64 as described above. Cells with either tail-Δ*AflII* expression plasmid displayed severe vacuole inheritance defects, whereas cells transformed with the vector were wild-type for vacuole inheritance (Fig. 5, B and C). These results suggest that the tail-Δ*AflII* competes with full-length Myo2p for binding to the vacuole, but not the essential cargo. Furthermore, this data is consistent with myo2-ΔAflIIp functioning for moving the vacuole, but not the essential cargo.

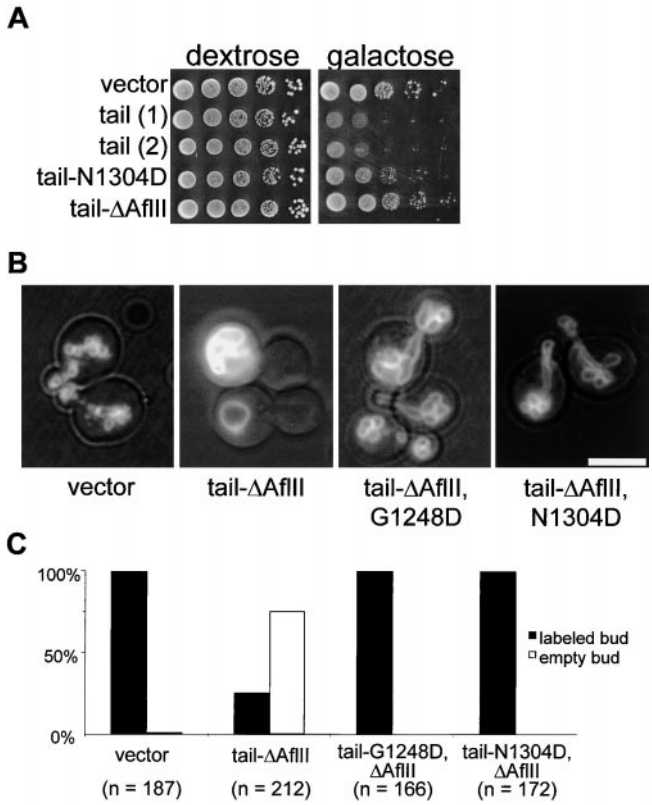

Figure 5. Overexpression of the Myo2p tail has dominant negative effects. A, Wild-type cells (LWY7235) were transformed with the following galactose-inducible expression plasmids: pYES2 (vector), pMYO2-tail (tail 1), pNLC60 (tail 2), pNLC59 (tail-N1304D), and pNLC22 (tail-Δ*AflII*). A dilution series of each transformant was spotted onto selective media containing dextrose or galactose. Cells overexpressing the tail domain with the Δ*AflII* 33-amino acid deletion are viable. B, Overexpression of the tail domain disrupts vacuole movement. LWY7235 cells were transformed with the following ADH-driven expression plasmids: pVT102-U (vector), pNLC27 (tail-Δ*AflII*), pNLC56 (tail-Δ*AflII*, G1248D), and pNLC57 (tail-Δ*AflII*, N1304D). Transformants were grown in selective media containing dextrose and labeled with FM4-64 to assess vacuole inheritance. Bar, 5 μm. C, Quantitation of vacuole inheritance in B.

In addition, we introduced G1248D (*myo2-2*) and N1304D mutations into these tail-Δ*AflII* constructs (pNLC56 and pNLC57, respectively). Although these mutant Myo2p tail domains are expressed to similar levels as tail-Δ*AflII* (pNLC27; data not shown), these constructs had no effects on vacuole inheritance. This data is consistent with these point mutations disrupting vacuole inheritance in the full-length *myo2* (Fig. 2).

Some HA-tail-ΔAflII Is Vacuole Associated

Shortly after induction, overexpressed Myo2p globular tail domain concentrates at sites of polarized growth, similar to full-length Myo2p (Reck-Peterson et al., 1999; Schott et al., 1999). Later, after higher levels of globular tail have been expressed, the tail localizes throughout the cell (Reck-Peterson et al., 1999). To investigate tail-Δ*AflII* localization, we performed double-label immunofluorescence in wild-type (LWY7235) cells containing pNLC45 (HA-tail-Δ*AflII*) using antibodies against HA and the vacuolar membrane protein, Vac8p (Wang et al., 1998). HA-tail-Δ*AflII* was distributed throughout the cell with apparent concentrations on the vacuole membrane (Fig. 6 A). Notably, no concentrations of HA-tail-Δ*AflII* at sites of polarized growth were observed. Cells containing pNLC27 (tail-Δ*AflII*) did not stain with HA antibody. We also performed single-label immunofluorescence using the HA antibody alone. These single-labeled cells also displayed a concentration of HA staining around what appears to be the vacuole (Fig. 6 B). This data suggests that some tail-Δ*AflII* localizes to the vacuole. Thus, the vacuole inheritance defect seen in tail-Δ*AflII* expressing cells may be due to interaction of this construct with Myo2p binding sites on the vacuole membrane.

Myo2p tail-ΔAflII Cofractionates with Full-length Myo2p

Previously, we found that the majority of Myo2p fractionated in the 13,000-*g* pellet (P13), which contains membranous organelles, including the vacuole (Catlett and Weisman, 1998). To examine further the localization of tail-Δ*AflII*, and to determine the effects of tail-Δ*AflII* overexpression on the distribution of full-length Myo2p, we fractionated extracts from wild-type (LWY7235) cells containing pNLC27 (tail-Δ*AflII*) by differential centrifugation. As observed previously, Myo2p fractionated primarily in the 13,000-*g* pellet (P13), with a small amount in the 100,000-*g* pellet (P100; Fig. 6 C). This fractionation pattern of Myo2p is seen in both cells expressing tail-Δ*AflII* and control cells containing the vector only (data not shown). The tail-Δ*AflII* fractionates like the full-length Myo2p, with the majority in the P13 (Fig. 6 C). This cofractionation of the tail-Δ*AflII* with the full-length Myo2p suggests the Myo2p tail domain is sufficient for this fractionation pattern.

We further explored effects of the tail-Δ*AflII* on Myo2p localization by isolating vacuoles from wild-type (LWY7235) cells containing pNLC27 (tail-Δ*AflII*) or the vector alone. Both full-length Myo2p and the tail-Δ*AflII* were found on vacuoles isolated from cells containing pNLC27 (Fig. 6 D). However, no obvious differences were seen in the amounts of full-length Myo2p on vacuoles isolated from cells containing pNLC27 or the vector (Fig. 6 D). This observation suggests that the inhibition of vacuole inheritance by tail-Δ*AflII* expression is not simply due to competitive inhibition of Myo2p binding to the vacuole.

Expression of Myo2p tail-ΔAflII Does Not Affect the Actin Cytoskeleton

Overexpression of the wild-type Myo2p tail causes abnormalities in the actin cytoskeleton, including actin bars and abnormally large actin patches (Reck-Peterson et al., 1999). Thus, we examined actin localization in cells overexpressing tail-Δ*AflII* by indirect immunofluorescence. Actin localization in cells expressing tail-Δ*AflII* was indistinguishable from cells carrying the vector alone (Fig. 7 A). No abnormal actin structures were seen in either strain. These observations suggest that the actin abnormalities seen in Myo2p tail–overexpressing cells result indi-

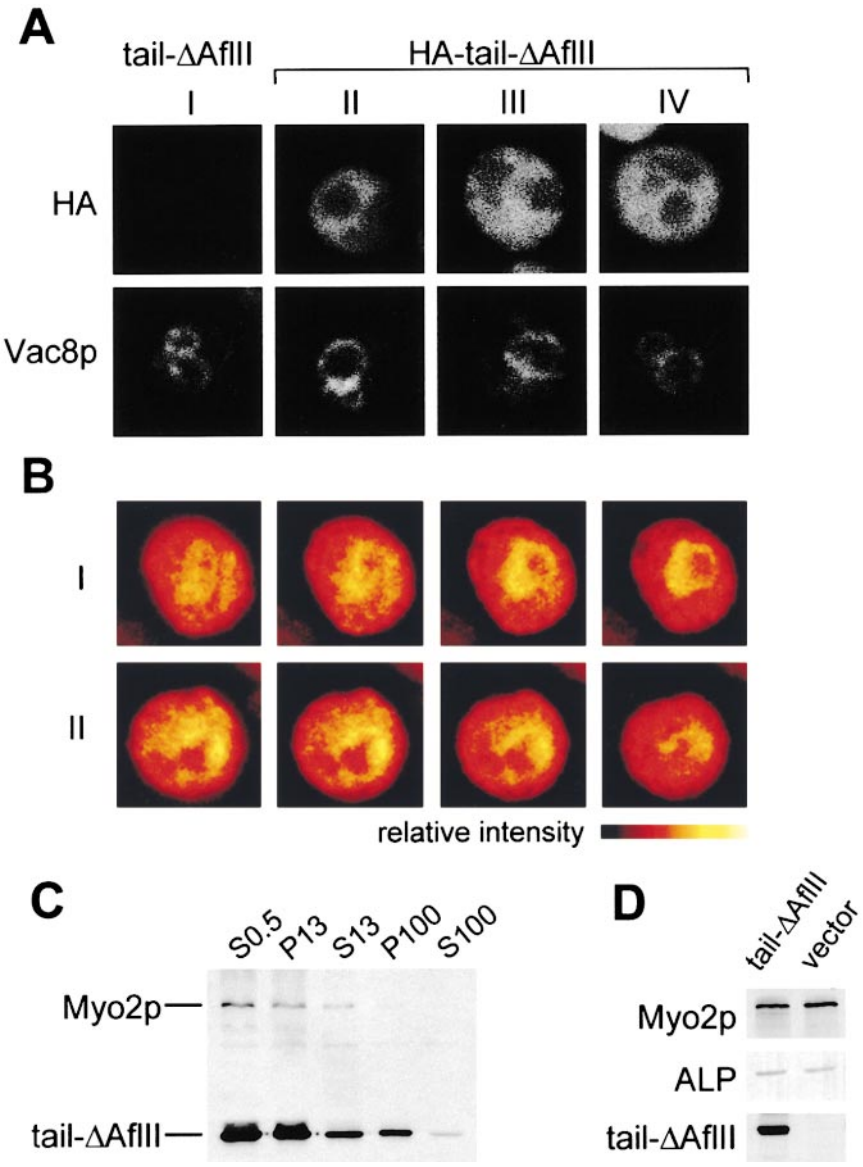

Figure 6. Immunolocalization of HA-tail-Δ*AflII*. Wild-type yeast (LWY7235) carrying a plasmid with tail-Δ*AflII* or HA-tail-Δ*AflII* were grown in selective media, fixed, and stained with anti-HA and anti-Vac8p antibodies (A) or anti-HA antibodies only (B). Images shown are individual sections from z-series obtained using confocal microscopy. B, I and II are series of sections spaced 0.5 μm apart. Images are pseudocolored to show relative intensity. C, Fractionation of tail-Δ*AflII*. LWY7235 cells carrying pNLC27 (tail-Δ*AflII*) were grown to log phase in selective media supplemented with 0.5% casamino acids. Cells were broken with glass beads and extracts centrifuged at 500 *g* to remove unbroken cells. The supernatant (S0.5) was further fractionated by differential centrifugation. Equal OD_{600} units of each fraction were separated by SDS-PAGE and transferred to nitrocellulose. Blots were probed with anti-Myo2p tail antibody. The majority of both Myo2p and tail-Δ*AflII* is found in the 13,000-*g* pellet (P13). D, Vacuoles were isolated on a Ficoll flotation gradient from LWY7235 cells carrying pNLC27 (tail-Δ*AflII*) or the vector plasmid. 5 μg protein from each sample was separated by SDS-PAGE and probed for Myo2p and the vacuolar membrane protein alkaline phosphatase (ALP).

rectly from disruption of the essential function(s) of Myo2p.

The Myo2p tail-ΔAflII Displaces Full-length Myo2p from Sites of Polarized Growth

One of the earliest phenotypes observed after induction of the Myo2p globular tail domain is displacement of the full-length Myo2p from sites of polarized growth (Reck-Peterson et al., 1999). Our results above (Fig. 4 C) indicate that the Δ*AflII* deletion does not affect localization of Myo2p. Accordingly, even though it does not affect polarized growth, expression of the tail-Δ*AflII* may disrupt polarized Myo2p localization. We investigated localization of full-length Myo2p by indirect immunofluorescence using an antibody directed against the motor domain of Myo2p (Reck-Peterson et al., 1999). At the same time, localization of HA-tail-Δ*AflII* was examined. As expected, wild-type (LWY7235) cells containing the vector plasmid displayed predominantly polarized localization of Myo2p (Fig. 7, B and C). In contrast, most cells containing pNLC45 (HA-tail-Δ*AflII*) had only punctate cytoplasmic Myo2p staining (Fig. 7, B and C). Moreover, HA staining indicated that the few cells displaying normal Myo2p polarization expressed little or no HA-tail-Δ*AflII* (not shown). These results show a strong correlation of tail-Δ*AflII* expression with mislocalization of the endogenous Myo2p.

Discussion

Current models for myosin-V function propose that the COOH-terminal globular tail domain binds to receptors on cargo organelles while the motor domain travels along actin filaments. Here, we describe two regions of the Myo2p globular tail domain, one involved in vacuole movement and one required for polarized growth. The identification of these two regions suggests that myosin-Vs bind different cargoes through interactions of distinct regions of the globular tail with organelle-specific receptors.

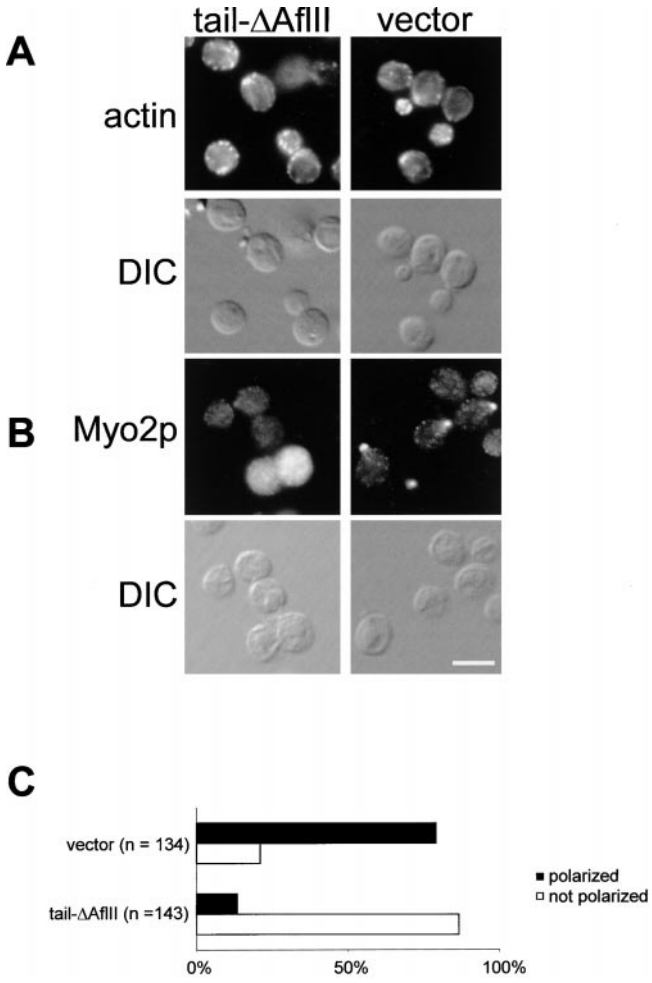

Figure 7. The Myo2p tail-Δ*AflII* displaces full-length Myo2p. LWY7235 (wild-type) cells containing pNLC45 (HA-tail-Δ*AflII*) or vector only were grown in selective media, fixed, and stained with antiyeast actin antibody (A) or anti-Myo2p motor domain antibody (B). Bar, 5 μm. C, Polarized Myo2p staining was assessed in unbudded and small-budded cells.

A Defined Region of the Myo2p Globular Tail Domain Is Required for Vacuole Inheritance

Through random mutagenesis of *MYO2*, we have identified a small region of the globular tail domain (amino acids 1,297–1,307) that is specifically required for vacuole movement. Mutations in any one of four amino acids in this region disrupt vacuole inheritance, but not polarized growth. Interestingly, this putative vacuole-binding region is predicted to be α-helical and the affected amino acids fall on the same face of this predicted helix. Thus, these new *myo2* mutations may affect vacuole inheritance by altering interactions of the Myo2p tail with a specific binding partner.

Because all of the potential mutants screened were derived from a single mutagenesis reaction, additional mutations of the Myo2p tail affecting vacuole inheritance may remain to be isolated. However, between the screen described in this report and an independent earlier screen that produced four *myo2* alleles with multiple amino acid changes (Table II), some degree of saturation has been obtained. Changes in D1297, N1304, and N1307 have each been isolated at least twice, either as different amino acid changes, or the same changes in independent screens. Moreover, *myo2-2* (G1248D) was isolated a second time.

The selection criteria used to obtain these mutants excluded both mutations that severely affected the essential function of Myo2p and those that only mildly affected vacuole inheritance. Thus, we would not expect to recover mutations that grossly disrupt the structure of Myo2p. Likewise, the mutations isolated do not appear to affect the stability or structure of Myo2p. Moreover, the vacuole inheritance defect is seen in these mutants at 24°C and no conditional growth phenotypes are present.

The Myo2p Globular Tail Contains Two Distinct Cargo-binding Domains

In addition to the putative vacuole-binding domain described, we identified a second region of the tail that is specifically required for polarized growth. This region is not required for vacuole inheritance or the polarized localization of Myo2p. *myo2*-Δ*AflII*, a deletion of amino acids 1,459–1,491, cannot support growth as the sole copy of Myo2p (Catlett and Weisman, 1998). However, *myo2*-Δ*AflII* can support vacuole inheritance in *myo2-2* cells (Fig. 4). These results suggest that the 1,459–1,491 deletion disrupts Myo2p interaction with secretory vesicles, but does not affect interaction with vacuoles.

In addition, overexpression of the tail-Δ*AflII* does not affect polarized growth like the wild-type tail (Fig. 5 A), but does severely inhibit vacuole movement (Fig. 5, B and C). These results are best explained by competition of the tail-Δ*AflII* with full-length Myo2p for factors required for movement of the vacuole, but not for movement of the essential cargo. Notably, point mutations of Myo2p affecting vacuole inheritance (G1248D and N1304D) block the effects of tail-Δ*AflII* on vacuole inheritance (Fig. 5, B and C). However, the exact mechanism for the negative effects on growth and vacuole inheritance caused by Myo2p tail and tail-Δ*AflII* overexpression is unclear. Reck-Peterson et al. (1999) found no effect of Myo2p tail overexpression on the fractionation pattern of full-length Myo2p. Similarly, while tail-Δ*AflII* fractionates in part with the vacuole, it does not significantly displace full-length Myo2p from the vacuole (Fig. 6 D). It is possible that the Myo2p interacts both nonspecifically with membranes and specifically with a protein receptor. Thus, tail-Δ*AflII* could disrupt productive interactions of full-length Myo2p with its vacuolar receptor, but not significantly alter Myo2p association with the vacuole.

During the preparation of this report, Schott et al. (1999) reported a screen for Myo2p tail mutants with conditional growth defects. None of these mutants displayed prominent defects in vacuole inheritance at either permissive or semipermissive temperatures, further supporting the existence of distinct cargo-binding regions for vacuoles and secretory vesicles. Through sequence comparison of Myo2p and other myosin-Vs and analysis of these multiple point mutants, Schott et al. (1999) propose two regions in the distal half of the Myo2p tail (1,389–1,427 and 1,439–1,478) as vesicle transport domains. Notably, the second of these regions overlaps with the deletion in *myo2*-Δ*AflII*. Inter-

estingly, both the proposed vacuole-binding and vesicle-binding domains fall in the AF-6/canoe homology region of the Myo2p tail (amino acids 1,225–1,501; Ponting, 1995).

Localization of Myo2p at Sites of Polarized Growth Is Not Required for the Essential Function

Myo2p concentrates at sites of polarized growth and this concentration has been presumed to reflect some function of Myo2p, such as organization of the actin cytoskeleton (Lillie and Brown, 1994) or the destination of Myo2p after delivery of cargo (Lillie and Brown, 1994; Schott et al., 1999). This concentration is at least in part dependent on transport along actin cables (Pruyne et al., 1998; Schott et al., 1999). However, the globular tail domain also appears to play a critical role. myo2-2p does not concentrate at sites of polarized growth, implying that the G1248D tail domain mutation affects a determinant for polarized Myo2p localization (Catlett and Weisman, 1998). Overexpression of the Myo2p globular tail domain displaces endogenous Myo2p from sites of polarized growth (Reck-Peterson et al., 1999). Further, tail-Δ*AflII* expression similarly disrupts localization of the endogenous Myo2p (Fig. 7, B and C) without affecting polarized cell growth. Thus, displacement of Myo2p by the tail does not occur through depolarization of the cell or impairment of vesicle transport to sites of Myo2p accumulation. Instead, the Myo2p tail may compete with the endogenous Myo2p for factors mediating polarized Myo2p accumulation. These observations support a model in which Myo2p moves along actin cables to sites of polarized growth and Myo2p localization at these sites is maintained via the tail domain.

The *myo2* vacuole inheritance mutants reported here display partial defects in the polarized concentration of Myo2p (Fig. 3). This is in sharp contrast to *myo2-2* (G1248D), a mutant severely defective in both vacuole inheritance and localization of Myo2p. Thus, at least three classes of Myo2p globular tail mutants exist: those defective in both vacuole inheritance and polarized Myo2p localization (*myo2-2*); those with vacuole inheritance defects, but only mild localization defects (*myo2-D1297G*, *myo2-D1297N*, etc.); and those affecting the essential function only (*myo2*-Δ*AflII*). This suggests that the tail may contain at least three functional cargo-binding or localization subdomains.

The coincidence of vacuole inheritance defects and Myo2p localization defects in our mutants is also consistent with a requirement for Myo2p concentration at polarized growth sites for vacuole inheritance. However, it is clear that polarized localization of Myo2p cannot be the major determinant of vacuole inheritance. First, as discussed above, there is no correlation in the severity of vacuole inheritance and Myo2p polarization defects. In addition, overexpression of the *myo2-66* suppressor, *SMY1* (Lillie and Brown, 1992), in *myo2-2* cells restores localization of the mutant Myo2p (Beningo et al., 2000), but not vacuole inheritance (Catlett, N.L, and L.S. Weisman, unpublished).

It remains unclear what the purpose of Myo2p concentration at sites of polarized growth is, as this localization appears unrelated to the essential function of Myo2p. Despite the absence of myo2-2p polarization, *myo2-2* cells grow relatively normally (Catlett and Weisman, 1998) and properly localize the secretory vesicle protein Sec4p to bud tips (Elkind et al., 2000). *myo2*-Δ*AflII* localizes normally (Fig. 4 C) despite its inability to support polarized growth (Catlett and Weisman, 1998). Moreover, conditional-lethal *myo2* mutants isolated by Schott et al. (1999) also display normal localization of the mutant Myo2p (Schott et al., 1999). This localization of Myo2p in the absence of polarized secretion indicates that polarized Myo2p concentration is not coupled to cargo binding and that perhaps this localization has an as yet unidentified, nonessential purpose.

How Do the Proposed Cargo-binding Regions Function?

The putative vacuole-binding region (amino acids 1,297–1,307) and *AflII* region (amino acids 1,459–1,491) may function by binding receptors on vacuoles and secretory vesicles, respectively. This cargo-specific receptor model best rectifies how mutations of different regions of the Myo2p tail affect different functions of Myo2p. Moreover, this model is consistent with the observed effects of overexpression of the globular tail domain and tail-Δ*AflII* on growth and vacuole inheritance. However, cargo receptors for Myo2p or any myosin-V remain to be identified.

Alternatively, these regions of the Myo2p globular tail may interact with proteins that regulate specific functions of Myo2p. A few potential regulators of Myo2p have been identified. The kinesin-like protein Smy1p suppresses both growth and localization defects of *myo2* mutants (Lillie and Brown, 1992, 1994; Schott et al., 1999; Beningo et al., 2000), but not vacuole inheritance defects (Catlett, N.L., and L.S. Weisman, unpublished data). Interaction of Smy1p with Myo2p is required for this suppression (Beningo et al., 2000), but Smy1p motor activity is not (Lillie and Brown, 1998). Hence, Smy1p may act to stabilize or otherwise regulate Myo2p interactions with secretory vesicles. Additionally, in animal cells, interaction of myosin-V with kinesin may coordinate microtubule and actin microfilament-based transport (Huang et al., 1999). A second potential Myo2p regulator is Rho3p, a Rho GTPase required for polarized growth. Rho3p interaction with Myo2p may regulate transport of secretory vesicles to the bud (Adamo et al., 1999). However, the Δ*AflII* region is not required for interactions of Myo2p with either Smy1p or Rho3p (Robinson et al., 1999; Beningo et al., 2000), so the growth defect of *myo2*-Δ*AflII* is not likely due to impaired interaction with these specific regulatory proteins.

We expect that these proposed cargo-binding regions may also be involved in posttranslational modification or conformational changes required for binding of specific cargoes. Phosphorylation has been reported to regulate *Xenopus laevis* myosin-V attachment to membranous cargo in a cell cycle-dependent manner (Rogers et al., 1999). It seems probable that phosphorylation and/or other posttranslational modifications regulate interactions of other myosin-Vs, including Myo2p, with specific cargoes.

Why would separate cargo-binding or regulatory domains be required for different functions of Myo2p? Secretory vesicles and the vacuole both undergo polarized transport, but the timing of transport and final destinations of these two cargoes are not identical. Before bud emergence, secretory vesicles target to the incipient bud

site. After budding, vesicles first polarize to the tip of small buds and then later switch to the entire bud surface. Then, before cytokinesis, vesicle transport shifts to the mother-bud neck (for review see Lew and Reed, 1995). The vacuole also polarizes to the incipient bud site in unbudded cells (Hill et al., 1996; Catlett and Weisman, 1998; Wang et al., 1998), and then a tubular or vesicular structure extends from the mother cell vacuole into the growing bud. However, this structure persists for less than half of the time between bud emergence and cytokinesis, and no vacuole movement is directed towards the mother-bud neck (Gomes de Mesquita et al., 1991). Distinct Myo2p receptors or regulatory proteins for secretory vesicles and the vacuole could facilitate the temporal and spatial regulation of transport required for these different transport processes.

We are grateful to Cheryl Bailey and Janet Hume for construction of pMYO2-tail and pRS416-MYO2-PEP4; John Nau, Jennifer Novak, and Emily Kauffman for excellent technical assistance; Samara Reck-Peterson, Peter Novick, and Mark Mooseker for generously sharing affinity-purified antibodies and plasmids; John Cooper for actin antiserum; David Weiss for critically reading the manuscript; and members of the Weisman lab, particularly Cecilia Bonangelino and Yong Xu Wang for helpful discussions.

Sequence data for *C. albicans* and *C. neoformans* were obtained from the Stanford DNA Sequencing and Technology Center website. Sequencing of *Candida albicans* was accomplished through support of the NIDR and the Burroughs Wellcome Fund.

This work was supported by the National Science Foundation career award MCB 96-00867 and the National Institutes of Health grant GM50403 to L.S. Weisman. N.L. Catlett was supported by the National Institutes of Health/National Institute on Aging grant T32 AG 00214 to the Interdisciplinary Research Training Program on Aging, University of Iowa.

Submitted: 18 January 2000
Revised: 26 May 2000
Accepted: 14 June 2000

References

Adamo, J.E., G. Rossi, and P. Brennwald. 1999. The rho GTPase rho3 has a direct role in exocytosis that is distinct from its role in actin polarity. *Mol. Biol. Cell*. 10:4121–4133.

Beningo, K.A., S.H. Lillie, and S.S. Brown. 2000. The yeast kinesin-related protein Smy1p exerts its effects on the class V myosin Myo2p via a physical interaction. *Mol. Biol. Cell*. In press.

Berkower, C., D. Loayza, and S. Michaelis. 1994. Metabolic instability and constitutive endocytosis of STE6, the a-factor transporter of *Saccharomyces cerevisiae*. *Mol. Biol. Cell*. 5:1185–1198.

Bonangelino, C.J., N.L. Catlett, and L.S. Weisman. 1997. Vac7p, a novel vacuolar protein, is required for normal vacuole inheritance and morphology. *Mol. Cell. Biol*. 17:6847–6858.

Bridgman, P.C. 1999. Myosin Va movements in normal and dilute-lethal axons provide support for a dual filament motor complex. *J. Cell Biol*. 146:1045–1060.

Catlett, N.L., and L.S. Weisman. 1998. The terminal tail region of a yeast myosin-V mediates its attachment to vacuole membranes and sites of polarized growth. *Proc. Natl. Acad. Sci. USA*. 95:14799–14804.

Cheney, R.E., M.K. O'Shea, J.E. Heuser, M.V. Coelho, J.S. Wolenski, E.M. Espreafico, P. Forscher, R.E. Larson, and M.S. Mooseker. 1993. Brain myosin-V is a two-headed unconventional myosin with motor activity. *Cell*. 75: 13–23.

Elkind, N.B., C. Walch-Solimena, and P.J. Novick. 2000. The role of the COOH terminus of Sec2p in the transport of post-Golgi vesicles. *J. Cell Biol*. 149: 95–110.

Evans, L.L., A.J. Lee, P.C. Bridgman, and M.S. Mooseker. 1998. Vesicle-associated brain myosin-V can be activated to catalyze actin-based transport. *J. Cell Sci*. 111:2055–2066.

Geourjon, C., and G. Deleage. 1995. SOPMA: significant improvements in protein secondary structure prediction by consensus prediction from multiple alignments. *Comput. Appl. Biosci*. 11:681–684.

Gomes de Mesquita, D.S., R. ten Hoopen, and C.L. Woldringh. 1991. Vacuolar segregation to the bud of *Saccharomyces cerevisiae*: an analysis of morphology and timing in the cell cycle. *J. Gen. Microbiol*. 137:2447–2454.

Gomes de Mesquita, D.S., H.B. van den Hazel, J. Bouwman, and C.L. Woldringh. 1996. Characterization of new vacuolar segregation mutants, isolated by screening for loss of proteinase B self-activation. *Eur. J. Cell Biol*. 71:237–247.

Govindan, B., R. Bowser, and P. Novick. 1995. The role of Myo2, a yeast class V myosin, in vesicular transport. *J. Cell Biol*. 128:1055–1068.

Hill, K.L., N.L. Catlett, and L.S. Weisman. 1996. Actin and myosin function in directed vacuole movement during cell division in *Saccharomyces cerevisiae*. *J. Cell Biol*. 135:1535–1549.

Huang, J.D., V. Mermall, M.C. Strobel, L.B. Russell, M.S. Mooseker, N.G. Copeland, and N.A. Jenkins. 1998. Molecular genetic dissection of mouse unconventional myosin-VA: tail region mutations. *Genetics*. 148:1963–1972.

Huang, J.D., S.T. Brady, B.W. Richards, D. Stenolen, J.H. Resau, N.G. Copeland, and N.A. Jenkins. 1999. Direct interaction of microtubule- and actin-based transport motors. *Nature*. 397:267–270.

Johnston, G.C., J.A. Prendergast, and R.A. Singer. 1991. The *Saccharomyces cerevisiae* MYO2 gene encodes an essential myosin for vectorial transport of vesicles. *J. Cell Biol*. 113:539–551.

Jones, E.W. 1991. Tackling the protease problem in *Saccharomyces cerevisiae*. *Methods Enzymol*. 194:428–453.

Kaiser, C., S. Michaelis, and A. Mitchell. 1994. Methods in Yeast Genetics. Cold Spring Harbor Laboratory Press, Cold Spring Harbor, NY.

Lew, D.J., and S.I. Reed. 1995. Cell cycle control of morphogenesis in budding yeast. *Curr. Opin. Genet. Dev*. 5:17–23.

Lillie, S.H., and S.S. Brown. 1992. Suppression of a myosin defect by a kinesin-related gene. *Nature*. 356:358–361.

Lillie, S.H., and S.S. Brown. 1994. Immunofluorescence localization of the unconventional myosin, Myo2p, and the putative kinesin-related protein, Smy1p, to the same regions of polarized growth in *Saccharomyces cerevisiae*. *J. Cell Biol*. 125:825–842.

Lillie, S.H., and S.S. Brown. 1998. Smy1p, a kinesin-related protein that does not require microtubules. *J. Cell Biol*. 140:873–883.

Long, R.M., R.H. Singer, X. Meng, I. Gonzalez, K. Nasmyth, and R.P. Jansen. 1997. Mating type switching in yeast controlled by asymmetric localization of ASH1 mRNA. *Science*. 277:383–387.

Mancini, A.J., L.S. Chan, and A.S. Paller. 1998. Partial albinism with immunodeficiency: Griscelli syndrome: report of a case and review of the literature. *J. Am. Acad. Dermatol*. 38:295–300.

Mercer, J.A., P.K. Seperack, M.C. Strobel, N.G. Copeland, and N.A. Jenkins. 1991. Novel myosin heavy chain encoded by murine dilute coat colour locus. *Nature*. 349:709–713.

Nascimento, A.A., R.G. Amaral, J.C. Bizario, R.E. Larson, and E.M. Espreafico. 1997. Subcellular localization of myosin-V in the B16 melanoma cells, a wild-type cell line for the dilute gene. *Mol. Biol. Cell*. 8:1971–1988.

Pastural, E., F.J. Barrat, R. Dufourcq-Lagelouse, S. Certain, O. Sanal, N. Jabado, R. Seger, C. Griscelli, A. Fischer, and G. de Saint Basile. 1997. Griscelli disease maps to chromosome 15q21 and is associated with mutations in the myosin-Va gene. *Nat. Genet*. 16:289–292.

Ponting, C.P. 1995. AF-6/cno: neither a kinesin nor a myosin, but a bit of both. *Trends Biochem. Sci*. 20:265–266.

Prekeris, R., and D.M. Terrian. 1997. Brain myosin V is a synaptic vesicle-associated motor protein: evidence for a Ca^{2+}-dependent interaction with the synaptobrevin–synaptophysin complex. *J. Cell Biol*. 137:1589–1601.

Provance, D.W., Jr., M. Wei, V. Ipe, and J.A. Mercer. 1996. Cultured melanocytes from dilute mutant mice exhibit dendritic morphology and altered melanosome distribution. *Proc. Natl. Acad. Sci. USA*. 93:14554–14558.

Pruyne, D.W., D.H. Schott, and A. Bretscher. 1998. Tropomyosin-containing actin cables direct the Myo2p-dependent polarized delivery of secretory vesicles in budding yeast. *J. Cell Biol*. 143:1931–1945.

Reck-Peterson, S.L., P.J. Novick, and M.S. Mooseker. 1999. The tail of a yeast class V myosin, Myo2p, functions as a localization domain. *Mol. Biol. Cell*. 10:1001–1017.

Robinson, N.G., L. Guo, J. Imai, E.A. Toh, Y. Matsui, and F. Tamanoi. 1999. Rho3 of *Saccharomyces cerevisiae*, which regulates the actin cytoskeleton and exocytosis, is a GTPase which interacts with Myo2 and Exo70. *Mol. Cell. Biol*. 19:3580–3587.

Rogers, S.L., R.L. Karcher, J.T. Roland, A.A. Minin, W. Steffen, and V.I. Gelfand. 1999. Regulation of melanosome movement in the cell cycle by reversible association with myosin V. *J. Cell Biol*. 146:1265–1276.

Rost, B., and C. Sander. 1994. Combining evolutionary information and neural networks to predict protein secondary structure. *Proteins*. 19:55–72.

Santos, B., and M. Snyder. 1997. Targeting of chitin synthase 3 to polarized growth sites in yeast requires Chs5p and Myo2p. *J. Cell Biol*. 136:95–110.

Schott, D., J. Ho, D. Pruyne, and A. Bretscher. 1999. The COOH-terminal domain of Myo2p, a yeast myosin V, has a direct role in secretory vesicle targeting. *J. Cell Biol*. 147:791–808.

Sikorski, R.S., and P. Hieter. 1989. A system of shuttle vectors and yeast host strains designed for efficient manipulation of DNA in *Saccharomyces cerevisiae*. *Genetics*. 122:19–27.

Takagishi, Y., S. Oda, S. Hayasaka, K. Dekker-Ohno, T. Shikata, M. Inouye, and H. Yamamura. 1996. The dilute-lethal (dl) gene attacks a Ca^{2+} store in the dendritic spine of Purkinje cells in mice. *Neurosci. Lett*. 215:169–172.

Thompson, J.D., D.G. Higgins, and T.J. Gibson. 1994. CLUSTAL W: improving the sensitivity of progressive multiple sequence alignment through se-

quence weighting, position-specific gap penalties and weight matrix choice. *Nucleic Acids Res.* 22:4673–4680.

van den Hazel, H.B., M.C. Kielland-Brandt, and J.R. Winther. 1993. The propeptide is required for in vivo formation of stable active yeast proteinase A and can function even when not covalently linked to the mature region. *J. Biol. Chem*. 268:18002–18007.

Vernet, T., D. Dignard, and D.Y. Thomas. 1987. A family of yeast expression vectors containing the phage f1 intergenic region. *Gene*. 52:225–233.

Vida, T.A., and S.D. Emr. 1995. A new vital stain for visualizing vacuolar membrane dynamics and endocytosis in yeast. *J. Cell Biol*. 128:779–792.

Walch-Solimena, C., R.N. Collins, and P.J. Novick. 1997. Sec2p mediates nucleotide exchange on Sec4p and is involved in polarized delivery of post-Golgi vesicles. *J. Cell Biol.* 137:1495–1509.

Wang, Y.X., N.L. Catlett, and L.S. Weisman. 1998. Vac8p, a vacuolar protein with armadillo repeats, functions in both vacuole inheritance and protein targeting from the cytoplasm to vacuole. *J. Cell Biol.* 140:1063–1074.

Wei, Q., X. Wu, and J.A. Hammer, 3rd. 1997. The predominant defect in dilute melanocytes is in melanosome distribution and not cell shape, supporting a role for myosin V in melanosome transport. *J. Muscle Res. Cell. Motil.* 18: 517–527.

Wu, X., B. Bowers, K. Rao, Q. Wei, and J.A.R. Hammer. 1998. Visualization of melanosome dynamics within wild-type and dilute melanocytes suggests a paradigm for myosin V function in vivo. *J. Cell Biol.* 143:1899–1918.